ZnO THIN FILMS BY PULSED LASER DEPOSITION WITH APPLICATIONS IN SENSORS

Izabela CONSTANTINOIU[1,2], Cristian VIESPE[3], Cristina BUSUIOC[4], Sorin-Ion JINGA[5]

ZnO was obtained by precipitation, sensitive thin films were deposited by Pulsed Laser Deposition and surface acoustic wave sensor was tested to different concentrations of hydrogen. ZnO powder was shaped by uniaxial pressing and sintered at 1200 ℃, thus obtaining a ceramic target for the ablation experiments. Thin films were deposited by pulsed laser deposition on quartz substrates, at 3 different pressures: 13.3, 93,3 and 173,3 Pa. The Scanning Electron Microscopy images indicated continuous and uniform films, the porous microstructures being more abundant with the increase of the deposition pressure. The X-Ray diffraction confirmed the ZnO deposition on the quartz substrate. The surface acoustic wave sensor was tested to hydrogen concentrations between 0.5-2% and its reversibility at room temperature was demonstrated.

Keywords: ZnO, precipitation, thin films, pulsed laser deposition, surface acoustic wave, sensors, room temperature, hydrogen.

1. Introduction

The progress of society has led to an increased need in the development of sensors due to the growing level of pollution, but also for control and safety in industry, medicine and transport. Consequently, researchers give a high importance to the development of sensors with good sensitivities, most precise selectivity depending on the field of application, short response time, repeatability and reversibility [1].

There is a wide range of sensors in continuous development: resistive sensors, surface acoustic wave sensors, chemoresistive sensors, electrochemical sensors, etc. [2-4]. They are used, depending on the sensitive material, for the

[1] PhD Student, Dept. Science and Engineering of Oxide Materials and Nanomaterials, The National University of Science and Technology POLITEHNICA Bucharest, Romania.
[2] Assistant researcher, Dept. Laser, National Institute for Laser, Plasma and Radiation Physics, Magurele, Romania.
[3] Scientific Researcher I, Dept. Laser, National Institute for Laser, Plasma and Radiation Physics, Magurele, Romania
[4] Associate Professor, Dept. Science and Engineering of Oxide Materials and Nanomaterials, The National University of Science and Technology POLITEHNICA Bucharest, Romania.
[5] Professor, Dept. Science and Engineering of Oxide Materials and Nanomaterials, The National University of Science and Technology POLITEHNICA Bucharest, Romania

detection of different types of gases, as volatile organic compounds, carbon dioxide, hydrogen, oxygen, hydrogen sulphide, ammonia or other potentially explosive, flammable or health-damaging gases [5-8]. Metal oxides (ZnO, SnO_2, WO_3, TiO_2, In_2O_3) [2, 9-12], metals (Pd, Pt, Cu, Au) [12-14] or polymers (polyethyleneimine, polymethylmethacrylate) [15, 16] are among the most used materials for the development of the sensitive component of sensors.

SAW sensors are in continuous development because of their advantages such as: high sensitivity and accuracy, fast response and return time, possibility of wireless operation, reliability and ease of fabrication, low cost, and the possibility to detect a large category of gases [1, 17]. More details about the sensor structure, operation and experimental testing can be found in section 2 of this work, Materials and Methods/Sensor Characterization.

ZnO is an important *n*-type semiconductor, used in many fields, with an excitation binding energy of 60 meV and a wide bandgap of 3.37 eV [18, 19]. It is frequently used due to the low cost, but also for the simplicity in the synthesis, through several methods: precipitation, sol-gel, chemical-vapour deposition, thermal decomposition, RF sputtering, etc [15, 20]. Other advantages of ZnO are chemical stability, possibility of doping, lack of toxicity and the ability of synthesis as various nanostructures, such as nanotubes, nanorods, nanowires, nanoflakes etc. [15, 21-23]. Its applications cover a wide range of fields, from the industrial environment to sensors, medicine and personal care [24].

ZnO is one of the materials with the greatest development potential in the field of sensors because of its high sensitivity, good physicochemical properties and fast response time [18, 25]. In the field of sensors, two of the disadvantages of ZnO relate to its low detection performance at room temperature (RT), but also to the lack of selectivity for most gases [18, 21]. The first one can be improved by using ZnO under different morphologies that increase its specific surface area, offering a larger interaction with gas molecules [2, 26, 27]. For the second one, it can be doped or used together with other materials with selective characteristics for a certain type of gas, as a composite [28, 29].

One of the simplest and inexpensive synthesis method for ZnO is precipitation. It is an inexpensive method that does not require a large consumption of resources, it is not time consuming and offers good control over particle composition [30, 31]. Pulsed laser deposition (PLD) is a fabrication method for thin films and different types of nanostructures, such as nanoparticles, nanowires, nanorods, nanoflakes, etc [32-34]. This method presents advantages such as the control of stoichiometry, a relatively high reproducibility, high deposition rate and the possibility to vary several deposition parameters to optimize the final properties of the film depending on the applications [35, 36]. Also, PLD is a method that can be used in different fields such as: sensors, biomaterials, electrocatalysis, optics, etc [28, 37-40]. Considering that the current performances obtained due to the

development of technology in different areas (electronics, communication, transport) are based on nanostructured materials, these methods can be successfully applied in the field of sensors to improve detection at RT.

This work combines the methods of precipitation and PLD, to optimize the morphological properties of ZnO films, for applications in gas sensors operating at RT. The novelty of our research resides in the development of a SAW sensor with ZnO sensitive layer, deposited by PLD at RT, with controlled morphology, for hydrogen detection at RT. The ease of fabrication and testing of this sensos, determines the perspective of fabricating other Zno SAW sensors with controlled morphology, through PLD, for better sensor performance.

2. Materials and Methods

2.1 Target Synthesis

ZnO was synthesized by precipitation. The precursors used were $Zn(NO_3)_2 \cdot 6H_2O$ (≥99%, Sigma Aldrich) and NaOH (Sigma Aldrich). $Zn(NO_3)_2 \cdot 6H_2O$ powder was dissolved in distilled water. The obtained solution was homogenized by magnetic stirring, producing its dissociation into Zn^{2+} and NO_3^-. A 2M NaOH solution was obtained by dissolving NaOH granules in the required amount of distilled water. During its homogenization, the dissociation into Na^+ and OH^- occurred. The precipitation was achieved by adding NaOH solution dropwise, up to a solution pH of 9. The homogenization continued for 1 h, after which the precipitate was filtered. During this time, the formation of $Zn(OH)_2$ as precipitate (Equation 1) [41] and $NaNO_3$ (Equation 2) [41] solution, took place. The filtrate was dried for about 4 h at 80 ℃ (Equation 3) [41]. The calcination was carried out at 600 ℃ for 2 h (Equation 4) [41].

$$Zn^{2+}_{(aq)} + 2OH^-_{(aq)} + xH_2O_{(aq)} \rightarrow Zn(OH)_2 \cdot xH_2O_{(s)} \downarrow \quad (1)$$

$$2Na^+ + 2NO_3^- \rightarrow 2NaNO_3 \quad (2)$$

$$Zn(OH)_2 \cdot x\,H_2O_{(s)} \downarrow \rightarrow Zn(OH)_{2\,(s)} + xH_2O_{(g)} \quad (3)$$

$$Zn(OH)_{2(s)} \rightarrow ZnO_{(s)} + H_2O_{(g)} \quad (4)$$

The next step was the granulation, for which a solution of 2 % polyvinyl alcohol (PVA) was used. A dense and wet mass was formed, which was three times passed through a very fine sieve after drying. The granulated powder was pressed into a 2,5 cm diameter cylindrical die, applying a pressure of 185 MPa, and after that, the target was sintered at 1200 ℃ for 2 h.

Going to thin films deposition by PLD, the ceramic target was placed in the deposition chamber on x-y tables controlled by computer, parallel to the substrate and at 40 mm distance from it. A Nd-YAG laser (EKSPLA NL301HT, Ekspla, Vilnius, Lithuania) was used, at 355 nm wavelength, 5 ns pulse duration,10 Hz frequency and 55 mJ energy per pulse. An oxygen atmosphere was maintained in

the deposition chamber, at different pressures, using a system consisting of a throttle valve (MKS 253B) controlled by a pressure controller (MKS 600) on a vane vacuum pump (Agilent Varian-DS602, Leini, Italy) and a mass-flow controller (MKS multigas 647) on the gas cylinders. The oxygen pressure was varied (13.3, 93,3 and 173,3 Pa), in order to observe how the morphology was influenced by it. The depositions were made on commercial single crystal quartz substrates (The Roditi International Corporation Ltd, London, England) at RT, using 36000 laser pulses.

2.2 Materials Characterization

After drying the precipitate, a thermal analysis was necessary to establish the appropriate calcination temperature. A Schimadzu DTG-60 equipment was utilized for this, in the temperature range 20-1000 ℃. The phase composition and crystalline structure of the materials in all three stages of synthesis were investigated by X-ray diffraction, using a Shimadzu XRD 6000 diffractometer with Ni filtered Cu Kα radiation (λ=0.154 nm), 2θ ranging between 10 and 80 °. By scanning electron microscopy (SEM), with a FEI QUANTA microscope, it was investigated the morphology of the samples. The thickness of the thin films was determined using a SURFCOM 180 A (Tokyo Seimitsu, Tokyo, Japan) profilometer.

2.3 Sensor Characterization

According to the image from Fig. 1, a SAW gas sensor (delay-line type) is made of a piezoelectric substrate, two pairs of interdigital transducers (IDT), a sensitive layer placed between the two pairs IDT, and gold wires to connect connection to the electrical source. In this work, a ST-X cut quartz piezoelectric substrate (The Roditi International Corporation Ltd, London, England) was used due to its stable temperature coefficient [1].

The IDT are made of gold (150 nm thickness) and have been deposited by photolithography on a chrome layer (60 nm thickness)) for a good adhesion. The configuration of the IDT was double comb and consists of 50 pairs of transducers.

An electrical input was applied on IDT, which was converted into surface acoustic waves due to the piezoelectricity of the substrate. The oscillation frequency of the waves that cross the sensor changes when the mass and/or acusto-electric characteristics of the sensitive layer change [1]. This frequency shift is processed by a specialized software and provides the response of the sensor.

The oscillation frequency of the sensor was approximately 69 MHz. It has a parallelogram geometry to reduce the effect of wave reflections, with the dimensions: 38 mm long, 10 mm wide and 0.5 mm thick.

The experimental setup for sensor tests is presented in Fig. 2 and it uses a CNT-91 Pendulum counter analyzer (Spectrocom Corp, Rochester, NY, USA) connected to a Time View 3 software (Pendulum Instruments, Banino, Poland).

The sensor tests were carried out at concentrations between 0.2 and 2% H_2, with a gas flow maintained at 0.5 l/min. These concentrations were obtained by combining a mixture of hydrogen (2% H_2/98% synthetic air) with pure synthetic air, using a system with mass-flow meters and mass-flow controllers (Fig. 2). More details about the test system used can be found in [28].

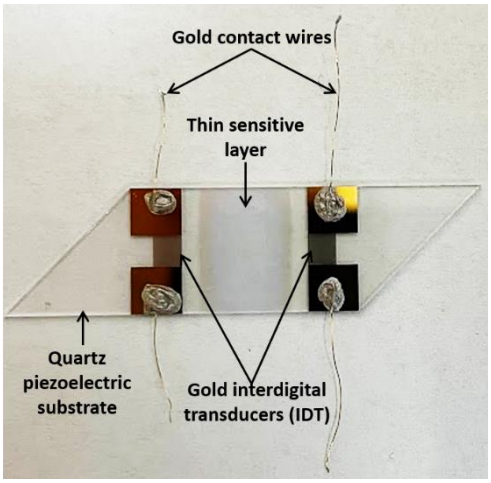

Fig. 1. Scheme of a SAW sensor.

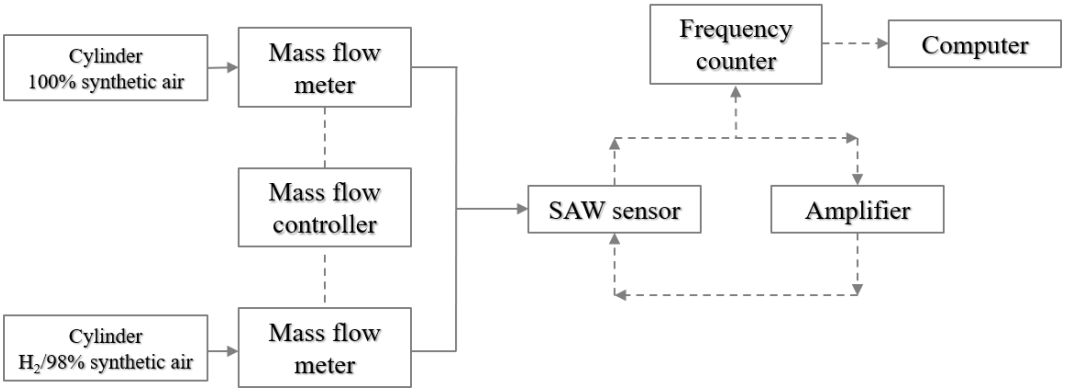

Fig. 2. Experimental setup for SAW sensor measurements.

3. Results and Discussions

Thermal analysis (Fig. 3), realised in 20-1000 ℃ range temperature, indicates that up to 600 ℃ there was the most important mass loss, until which all gas generating components have been eliminated, and this was established as calcination temperature.

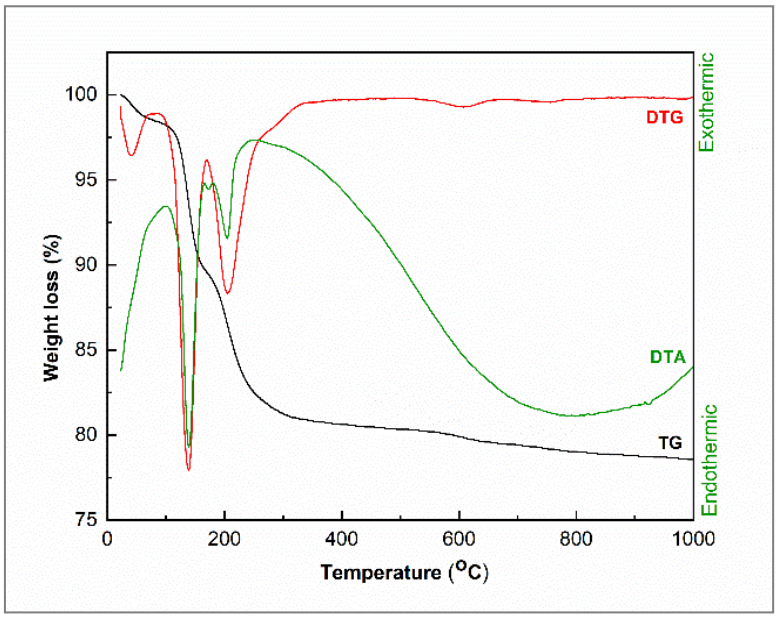

Fig. 3. Thermal analysis of the precipitate: TG - thermogravimetric analysis, DTG - the derivative of the thermogravimetric analysis with respect to time and DTA - differential thermal analysis.

The compositional and structural evaluation of the samples after the three different thermal treatments (drying, calcination and sintering) led to the XRD patterns presented in Fig. 4. The XRD pattern recorded after drying at 80 ℃ indicates the presence of a majority phase of $Zn(OH)_2$ (ICDD 00-012-0479) in the orthorhombic system, P212121 space group and a minority phase of ZnO (ICDD 00-080-0075) in the hexagonal system and P36mc space group. After calcination at 600 ℃, the system remains composed of a single phase, hexagonal ZnO (ICDD 00-080-0075) in P63mc space group. Increasing the temperature at 1200 ℃, ZnO structure remains hexagonal, in P36mc space group (ICDD 00-080-0075), with sharp and narrow peaks, showing that the powder is composed of small sized crystallites. Using Scherrer equation (Equation 5), the average crystallite size (D) of the ZnO phase was calculate for each heat treatment step, resulting the following values: 23 nm after drying at 80 ℃, 37 nm after calcination at 600 ℃ and 38 nm after sintering at 1200 ℃. It was observed that this parameter obviously increased after calcination, being approximately constant after sintering.

$$D = \frac{K\lambda}{\beta cos\theta} \tag{5}$$

where K is the Scherrer constant (0.9), λ is the wavelength of X-ray radiation (0.154 nm), β is the full width at half maximum of the peak and θ is the Bragg angle.

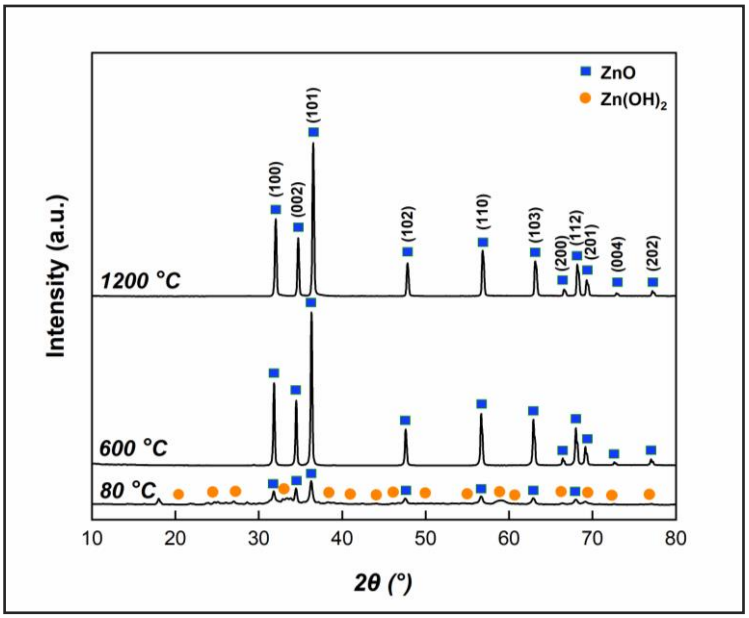

Fig. 4. XRD patterns of the samples after the three thermal treatments.

The SEM images in Fig. 5 reveal specific morphologies of ZnO [15] after drying and calcination, respectively. After drying at 80 °C (Fig. 5a), agglomerations with irregular shapes and sizes are observed, predominating the platelet and acicular particles. After calcination at 600 °C (Fig. 5b), the shape of the particles changed, becoming predominantly spherical, with different sizes.

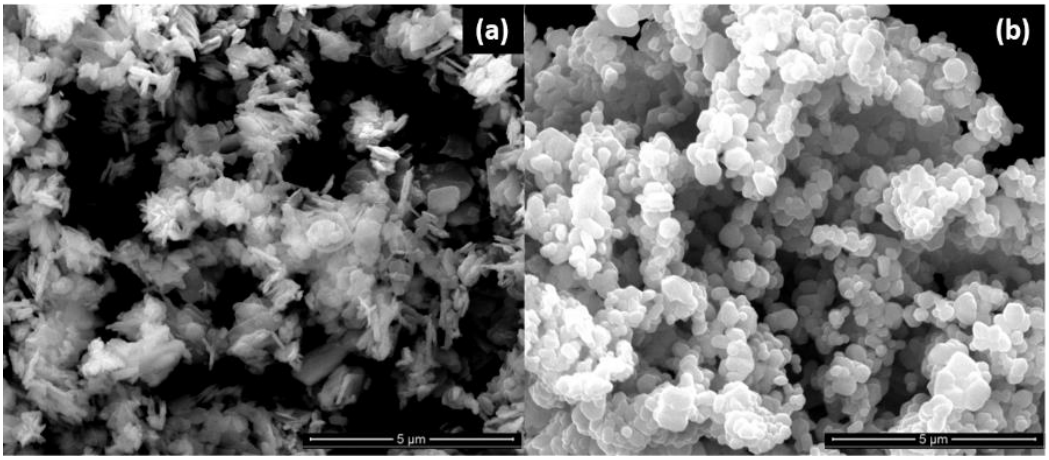

Fig. 5. SEM images of: (a) the precipitate dried at 80 °C and (b) the powder calcined at 600 °C.

The purpose of the material obtained in this work was to be deposited as a thin film for applications in gas sensing, for RT detection. For different sensors, the sensitive film needs to meet certain criteria to achieve best performance. One of the frequently encountered criteria is the morphology of the sensitive film [12]. For example, in the case of surface acoustic wave sensors, a stable, continuous and uniform layer is needed, but also a porous layer to increase the area of interaction between the gas molecules and the sensitive layer [12, 35]. A porous film also favours detection at RT, due to the increased sensitivity. Considering that a large category of sensors needs thermal energy to provide response, in order to save energy consumed in detection and to simplify the operation system of the sensor, the possibility of RT detection is being studied, by developing sensitive porous thin films.

From ZnO target obtained (Fig. 6), thin films were deposited at different oxygen pressures so as to observe how this parameter influences the morphology of the films on quartz substrates. The pressures were 13.3, 93,3 and 173,3 Pa. The SEM images for these thin films can be found in Fig. 7. The first aspect observed was that the deposited films are continuous and uniform (Fig. 7a, c, e). It was also remarked that with the increase of deposition pressure, on the surface of the film appear droplets and different porous structures, formed by agglomerations of ZnO grains. Images b, d, and f from Fig. 7 show the formation of three distinct morphologies. The film deposited at 13.3 Pa (Fig. 7b) consists of nano-sized wire-like formations. This type of morphology fulfils the criteria for ensuring a large specific surface area for applications in sensors. Increasing the pressure to 93.3 Pa (Fig. 7f), a layer consisting of grains and agglomerations of grains of different shapes and sizes can be observed. It is a stable layer, which can be successfully used as sensitive layer for sensors, if the benefit brought by the large specific surface area is greater than the disadvantage given by the noise induced by the droplets. When the oxygen pressure is 173.3 Pa, the morphology changes considerably. On the surface of the film, agglomerations of grains are observed, which favour the development of a porous morphology. They significantly increase the interaction surface area of the thin film and the gas molecules, leading to much better sensor results. It was demonstrated that with the increase of porosity and surface roughness, the performance of the sensors increases because of the large surface area [12, 28]. However, to ensure the functioning of the sensor, the sensitive film needs to be stable on the substrate and with an optimal thickness. Thus, there is a need to study the behaviour of materials at different deposition pressures.

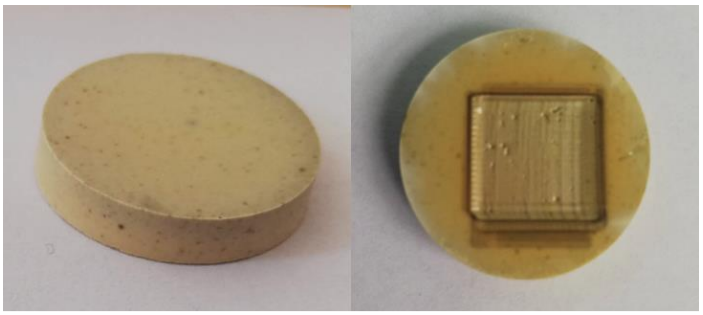

Fig. 6. ZnO target before and after PLD deposition.

The different morphology of the films, triggered by the variable oxygen pressure, is explained by the hydrodynamic effects resulting from the collision of the ablated species with the molecules of gas at high pressures [28]. These effects lead to the slowing of the species in plasma, they remain in the area between the target and the substrate for a longer time, which favours nucleation in the gas phase. Such nucleation leads to the formation of nanoparticles in this area, supporting in this way the porous morphology [35, 42]. Considering the aspects discussed, all three films can be used for applications in gas sensors. However, the film deposited at 173.3 Pa showed the greatest potential in obtaining the highest sensitivity and the lowest limit of detection.

XRD pattern on the film deposited at 13.3 Pa in Fig. 8, confirms the deposition of ZnO wurtzite structure (ICDD 96-900-8878), in hexagonal system, P63mc space group. As well, it can be stated that the use of these two synthesis methods, precipitation and PLD, offers the possibility of developing optimal sensitive layers for SAW sensors.

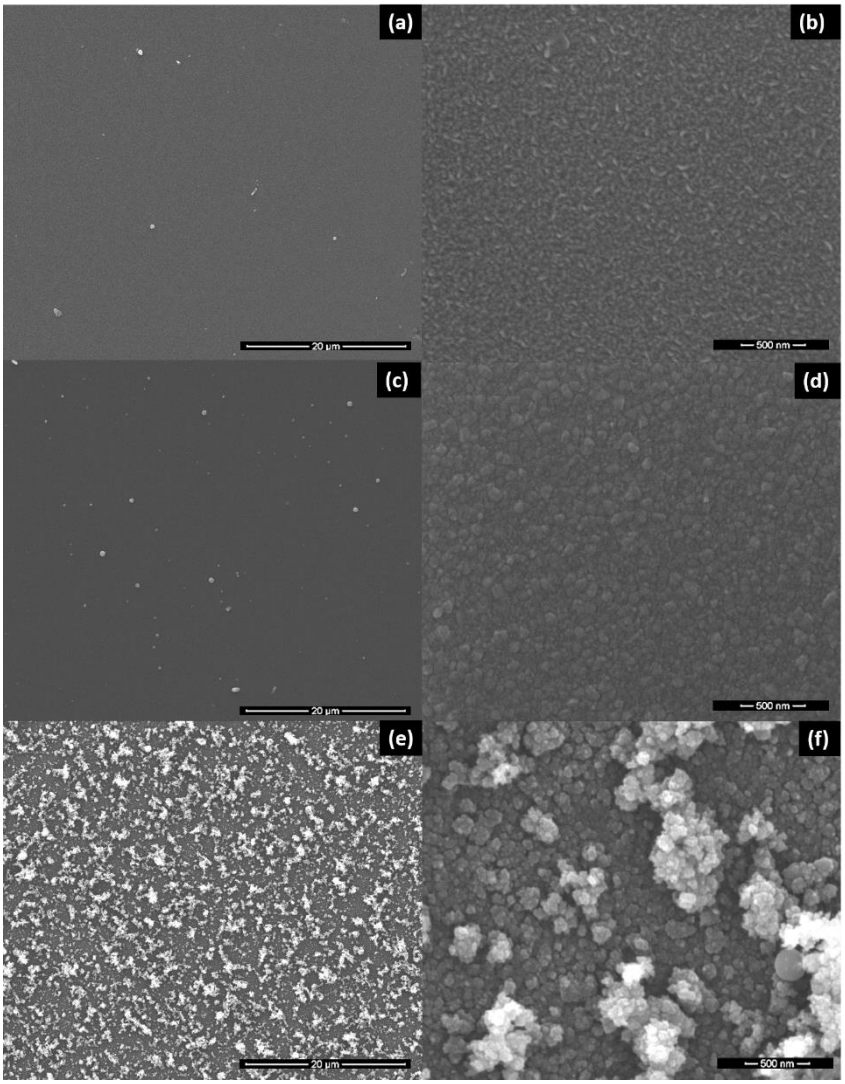

Fig. 7. SEM images of PLD thin films deposited at: (a and b) 13.3 Pa, (c and d) 93.3 Pa and (e and f) 173.3 Pa oxygen pressure.

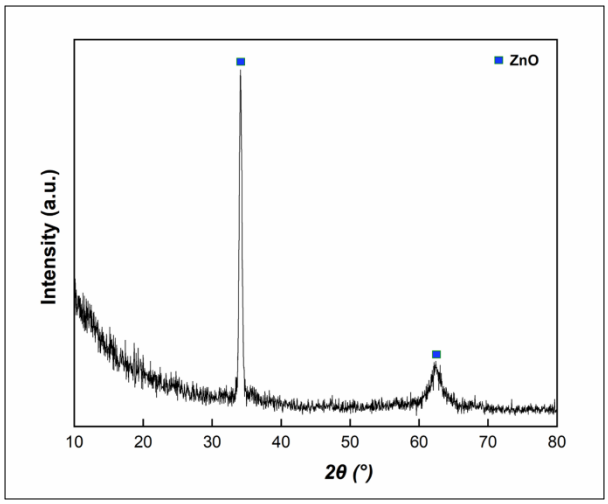

Fig. 8. XRD pattern of the thin film deposited at 13.3 Pa.

The influence of pressure on the thickness of the thin films deposited at the three different oxygen pressures was studied. The following film thicknesses were obtained: 650 nm for the 13.3 Pa oxygen pressure, 363 nm for the 93.3 Pa oxygen pressure, 150 nm for the 173.3 Pa oxygen pressure. Although the expectation was that with the increase of oxygen pressure, the thickness of the films increases, the results showed that the thickness of the films decreases with the increase of oxygen pressure. It was demonstrated that above oxygen pressures of 1.3 Pa, the tendency of the thickness of the films is to decrease due to the kinetic energy of the atoms in plasma plume, which decreases due to stronger and numerous interactions with the gas molecules [43]. This energy decrease of the atoms leads to the slowing down of the possibility to form low energy structure. It can also be seen from the SEM images (Fig. 7) that at 173.3 Pa, it was not formed a structure with high porosity so that it could influence the film thickness. Taking into account these aspects and the intended application for the deposited films, it is necessary to optimize the oxygen pressure to obtain the designed performances.

The layer deposited at 93.3 Pa O_2 pressure was chosen to verify the applicability of these thin films as sensitive layers for SAW sensors. The tests were carried out for different hydrogen concentrations. Hydrogen is of great interest for replacing fossil fuels and thus protecting the environment. However, it has some disadvantages, one of them being that it becomes explosive at concentrations between 4%-75% (0.60 cm^2/s diffusion coefficient in air) [12, 28]. Being a colourless and odourless gas, with a high capacity to penetrate many environments, it requires the development of efficient sensors for a safe use [12].

The sensor was tested at concentrations between 0.5-2% hydrogen and it responded at each concentration tested. The noise level (n) during tests was 6 Hz.

In Fig. 9, it is clearly observed that the frequency shift was more pronounced with the increase of hydrogen concentration tested. The average sensibility calculated (Table 1) was 0.0119 Hz/ppm and the limit of detection (LOD) was 1515.47 ppm. These results are comparable or better than other results from the literature for hydrogen detection with SAW sensors, but for which structures from several types of materials or the development of complicated microstructures were needed [2, 12, 44]. The reversibility of the sensor was also demonstrated, as it is indicated in the dynamic response in Fig. 10. The sensor responded at RT, and its desorption took place at RT. Taking into account that both the deposition of the sensitive layer and the testing process were carried out at RT, these results are precursors to the development of SAW sensors with great sensitivity, LOD and with low energy consumption and ease of implementation.

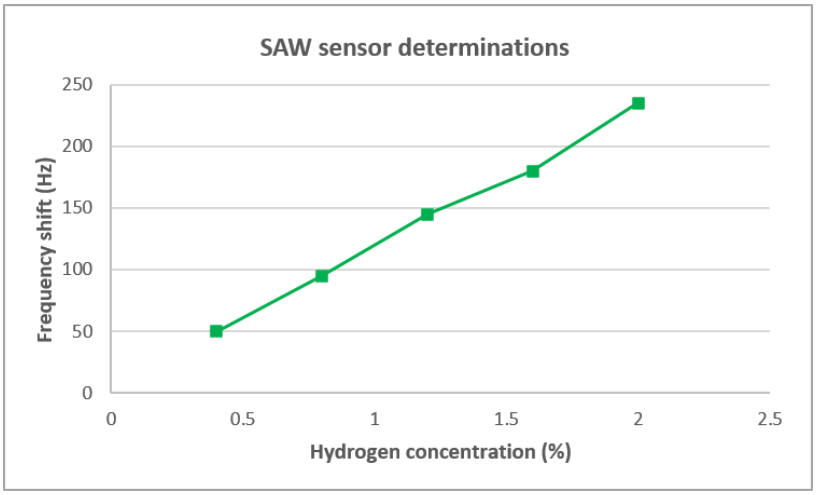

Fig. 9. SAW sensor frequency shift for different hydrogen concentration.

Table 1.

Frequency shift, sensitivity and limit of detection (LOD) of the sensor (Δf-frequency change; c-hydrogen concentration, *n*-noise level).

Hydrogen concentration (ppm)	Frequency shift (Hz)	Sensitivity (Δf/c) (Hz/ppm)	LOD (3x*n*)/(Δf/c) (ppm)
4000	50	0.0125	1440
8000	95	0.0119	1516
12000	145	0.0121	1490
16000	180	0.0113	1600
20000	235	0.0118	1532
Average		**0.0119**	**1516**

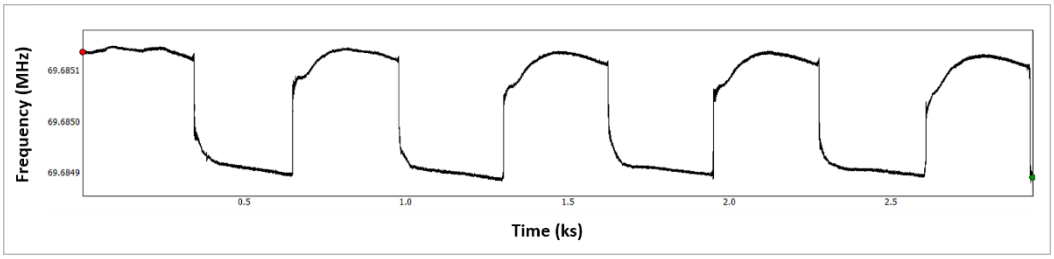

Fig. 10. Dynamic response of SAW sensor for 0.8% hydrogen concentration.

4. Conclusions

ZnO was synthesized by the precipitation method, with hexagonal structure and P36mc space group. It was sintered at 1200 ℃ as a ceramic target. PLD depositions were made varying the oxygen pressure at 13.3, 93,3 and 173,3 Pa. SEM images of the thin films deposited on quartz showed the deposition of stable, continuous and uniform films. Moreover, with the increase of the deposition pressure, the presence of droplets was identified, while at 173.3 Pa, porous microstructures were formed.

A SAW sensor with ZnO sensitive layer deposited at 93.3 Pa O_2 pressure was fabricated. It was tested at RT, at hydrogen concentrations between 0.5-2% and results were obtained for all concentrations. The average calculated sensitivity was 0.012 Hz/ppm and the LOD had an average value of 1516 ppm. Also, through successive tests at 800 ppm hydrogen concentration, it was demonstrated thet the sensor is reversible at RT.

These results are precursors to the development of SAW sensors with excellent performances at RT for hydrogen detection, which offer both ease of implementation, low energy consumption and reliability. One of the next perspectives is to explore a higher range of PLD parameters that can influence the properties of ZnO films and obtaining different types of morphology that will facilitate hydrogen detection. Also, SAW sensors with such layers can be tested for other gases.

Acknowledgement

This research was supported by Romanian Ministry of Research, Innovation and Digitization under Romanian National Core Program LAPLAS VII – contract no. 30N/2023.

REFERENCES

[1]. D. S. Ballentine, R.M. White, S. J. Martin, A. J. Ricco, E. T. Zellers, C. G. Frye, H. Wohtjen, Acoustic Wave Sensors, Theory, Design, and Physico-Chemical Applications, Academic Press: San Diego, CA, USA, 1997.
[2]. I. Constantinoiu, D. Miu, C. Viespe, SAW Hydrogen Sensors with Pd/SnO2 Layers, Materials, vol 15, no 8012, 2022.
[3]. A. Ferlazzo, C. Espro, D. Iannazzo, K. Moulaee, G. Neri, A novel yttria-doped ZrO2 based conductometric sensor for hydrogen leak monitoring, International Journal of Hydrogen Energy, vol 47, 2022, pp. 9819–9828.
[4]. S. Zhang, C. Yin, L. Yang, Z. Zhang, Z. Han, Investigation of the H2 sensing properties of multilayer mesoporous pure and Pd-doped SnO2 thin film, Sensors and Actuators B-Chemical, vol 283, 2019, pp. 399–406.
[5]. S. Dey, G.C. Dhal, Materials progress in the control of CO and CO2 emission at ambient conditions: an overview, Materials Science for Energy Technologies, vol. 2, 2019, pp. 607-623.
[6]. A. S. Lagutin, A. A. Vasilev, Solid-State Gas Sensors, Journal of Anaytical Chemistry, vol 77, no 2, 2022, pp 131-144.
[7]. I. Constantinoiu, D. Miu, C. Viespe, Surface Acoustic Wave Sensors for Ammonia Detection at Room Temperature Based on SnO2/Co3O4 Bilayers, Journal of Sensors, Vol 2019, 2019, article ID: 8203810.
[8]. I. Constantinoiu, C. Viespe, Hydrogen Detection with SAW polymer/quantum dots sensitive films, vol 19, no 4481, 2019.
[9]. M.Y. Arsent'ev, M.V. Kalinina, N. Koval'ko, T.L. Simonenko, L.V. Morozova, P.A. Tikhonov, O.A. Shilova, Inorganic Materials: Applied Research, vol. 11, no. 2, 2020, pp. 441.
[10]. A. Staerz, S. Somacescu, M. Mauro, T. Russ, U. Weimar, N. Barsan, WO3 Based Gas Sensors, Proceedings, vol. 2, 2018, 826.
[11]. Z. Yu, J. Gao, L. Xu, T. Liu, X. Wang, H. Suo, C. Zhao, Fabrication of lettuce-like ZnO gas sensors with enhanced H2S gas sensitivity, Crystals, vol. 10, no. 3, 2020, pp. 145.
[12]. I. Constantinoiu, C. Viespe, Development of Pd/TiO2 porous layers by pulsed laser deposition for surface acoustic wave H2 gas sensor, Nnaomaterials, vol 10, 2020, 760.
[13]. S. Öztürk, N. Kılınç, Pd thin films on flexible substrate for hydrogen sensor. Journal of Alloys and Compounds, vol 674, 2016, pp. 179–184.
[14]. C. Viespe, V. Dinca, G. Popescu-Pelin, D. Miu, Love wave surface acoustic wave sensor with laser-deposited nanoporous gold sensitive layer, vol 19, no 20, 2019, pp. 4492.
[15]. I. Constantinoiu, C. Viespe, ZnO metal oxide semiconductor in surface acoustic wave sensors: A review, Sensors, vol 20, 2020, 5118.
[16]. A. Saaedi, P. Shabani, R. Yousefi, High performance of methanol gas sensing of ZnO/PAni nanocomposites synthesized under different magnetic field. Journal of Alloys and Compounds vol 802, 2019, pp. 335–344.
[17]. D. Mandal, S. Banerjee, Surface Acoustic Wave (SAW) Sensors: Physics, Materials and Applications, Sensors, vol 22, no. 820, 2022.
[18]. J. Ding, H. Dai, H. Chen, Y. Jin, H. Fu, B. Xiao, Highly sensitive ethylene glycol gas sensor based on ZnO/rGO nanosheets, Sensors and Actuators: B. Chemical, vol 372, 2022, 132655.
[19]. K. Das, B. Jana, M. Pramanik, M. Mallick, J. Das, J. Sengupta, Chemically synthesized ZnO nanocrystal-based ethylene sensor operative at natural humid condition, Applied Physics A, vol 128, no 962. 2022.
[20]. L. Motelica, O. C. Oprea, B. S. Vasile, A. Ficai, D. Ficai, E. Andronescu, A. M. Holban, Antibacterial Activity of Solvothermal Obtained ZnO Nanoparticles with Different

Morphology and Photocatalytic Activity against a Dye Mixture: Methylene Blue, Rhodamine B and Methyl Orange, Internatinal Journal of Molecular Science, vol 24, no. 5677, 2023.
[21]. M. Yang, S. Zhang, F. Qu, S. Gong, C. Wang, L. Qiu, M. Yang, W. Cheng, High performance acetone sensor based on ZnO nanorods modified by Au nanoparticles, vol 797, 2019, pp. 246-252.
[22]. Z. Shen, X. Zhang, X. Ma, Y. Chen, M. Liu, C. Chen, S. Ruan, Synthesis of hierarchical 3D porous ZnO microspheres decorated by ultra-small Au nanoparticles and its highly enhanced acetylene gas sensing ability, J. Alloy. Comp. 731 (2018) 1029e1036.
[23]. N. A. Patel, I. B. Patel, V. L. Bharat, Structural, thermal and chemical studies of Mn doped ZnO nanoparticles synthesized by co-precipitation method, Materials Today: Proceedings, vol 46, 2021, pp. 2277-2280.
[24]. L. Motelica, B. S. Vasile, A. Ficai, A. V Surdu, D. Ficai, O. C. Oprea, E. Andronescu, D. C. Jinga, A. M. Holban, Influence of the Alcohols on the ZnO Synthesis and Its Properties: The Photocatalytic and Antimicrobial Activities, Pharmaceutics, vol 14, no. 2842, 2022.
[25] S. Narasimman, L. Balakrishnan, Z. C. Alex, Fiber-optic ammonia sensor based on amine functionalized ZnO nanoflakes, IEE Sensors Journal, vol 18, no 1, January 2018, pp 201-208.
[26]. H. Chai, Z. Zheng, K. Liu, J. Xu, K. Wu, Y. Luo, H. Liao, M. Debliquy, C. Zhang, Stability of Metal Oxide Semiconductor Gas Sensors: A Review, IEE Sensors Journal, vol 22, no 6, March 2022, pp. 5470-5481.
[27]. G. Fedorenko, L. Oleksenko, N. Maksymovych, Oxide Nanomaterials Based on SnO2 for Semiconductor Hydrogen Sensors. Advances in Materials Science and Engineering, 2019, 5190235.
[28]. D. Miu, I. Constantinoiu, C. Enache, C. Viespe, Effect of Pd/ZnO morphology on surface acoustic wave sensor response, Nanomaterials, vol 22, 2598, 2021.
[29]. D. Li, X. Le, J. Pang, L. Peng, Z. Xu, C. Gao, J. Xie, A SAW hydrogen sensor based on decoration of graphene oxide by palladium nanoparticles on AIN/Si layered structure. Journal of Micromechanics and Microengineering vol. 29, 2019, 45007.
[30]. N.A. Yazid, Y.C. Joon, Co-precipitation synthesis of magnetic nanoparticles for efficient removal of heavy metal from synthetic wastewater. AIP Conference Proceedings. Vol 2124, 2019, 020019.
[31]. U.P.M. Ashik, S. Kudo, J. Hayashi, Chapter 2—An Overview of Metal Oxide Nanostructures. In Synthesis of Inorganic Nanomaterials; S.M. Bhagyaraj, O.S. Oluwafemi, N. Kalarikkal, S. Thomas, Eds.;Woodhead Publishing: Philadelphia, PA, USA, 2018; pp.19–57.
[32]. A. L. Nikolaev, A. S. Kamencev, N. V. Lyanguzov, S. M. Aizikovich, Pulsed laser deposition of Au nanoparticles on ZnO nanostructures, IOP Conf. Series: Materials Science and Engineering, vol. 1029, no. 012064, 2021.
[33]. K. Eng Ng, T. Y. Tiong, M. Mohamed, W. S. Chang, C. Fu Dee, B. Majlis, Synthesis of ZnO nanoflakes by 1064 nm Nd:YAG pulsed laser deposition in a horizontal tube furnace, 018 IEEE International Conference on Semiconductor Electronics (ICSE), Kuala Lumpur, Malaysia, 2018, pp. 140-143, doi: 10.1109/SMELEC.2018.8481292.
[34]. B. ElZein, Y. Yao, A. S. Barham, E. Dogheche, G. E. Jabbour, Toward the Growth of Self-Catalyzed ZnO Nanowires Perpendicular to the Surface of Silicon and Glass Substrates, by Pulsed Laser Deposition, Materials, vol. 13, no. 4427, 2020.
[35]. P. Cheng, L. Wang, Y. Pan, H. Yan, D. Gao, J. Wang, H. Zhang, Fiber Bragg grating temperature sensor of cladding with SrTiO3 thin film by pulsed laser deposition, Laser Physics, vol 29, 2019, 25107.
[36]. I. Constantinoiu, C. Viespe, Synthesis Methods of Obtaining Materials for Hydrogen Sensors, Sensors, vol 21, 2021, 5758.

[37]. C. Busuioc, G. Voicu, I.D. Zuzu, D. Miu, C. Sima, F. Iordache, S.I. Jinga, Vitroceramic coatings deposited by laser ablation on Ti-Zr substrates for implantable medical applications with improved biocompatibility, Ceramics International, vol 43, 2017, pp. 5498–5504.
[38]. G. Voicu, D. Miu, I. Dogaru, S. I. Jinga, C. Busuioc, Vitroceramic interface deposited on titanium substrate by pulsed laser deposition method, International Journal of Pharmaceutics, vol. 510, 2016, pp. 449–456.
[39]. X. Du, H. Ai, M. Chen, D. Liu, S. Chen, X. Wang, K. H. Lo, H. Pan, PLD-fabricated perovskite oxide nanofilm as efficient electrocatalyst with highly enhanced water oxidation performance, Applied Catalysis B: Environmental vol. 272, 2020, pp. 119046.
[40]. J. Winiger, K. Keller, D. Moor, M. Baumann, D. Kim, D. Chelladurai, M. Kohli, T. Blatter, E. Dénervaud, Y. Fedoryshyn, U. Koch, S. Pané, R. Grange, J. Leuthold, PLD Epitaxial Thin-Film BaTiO3 on MgO − Dielectric and Electro-Optic Properties, Advanced Materials Interfaces, no. 2300665, 2023.
[41]. M. G. Kotresh, M. K. Patil, S. R. Inamdar, Reaction temperature-based synthesis of ZnO nanoparticles using co-precipitation method: Detailed structural and optical characterization, Optik, vol 243, 2021, 167506.
[42]. D. B. Geohegan, A. A. Puretzky, Laser ablation plume thermalization dynamics in background gases: Combined omaging, optical absorption and emission spectroscopy, and ion measurements, Applied Surface Science, vol 96-98, 1996, 131-138.
[43]. Z. G. Zhang, F. Zhou, X. Q. Wei, M. Liu, G. Sun, C.S. Chen, C.S. Xue, H. Z. Zhuang, B. Y. Man, Effects of oxygen pressures on pulsed laser deposition of ZnO films, Physica E, vol 39, 2007, 253-257.
[44]. A. Marcu, C. Viespe, Surface Acoustic Wave Sensors for Hydrogen and Deuterium Detection, Sensors, vol. 17, no. 1417, 2017.